



This discussion paper is/has been under review for the journal Hydrology and Earth System Sciences (HESS). Please refer to the corresponding final paper in HESS if available.

Soil buffer limits flash flood response to extraordinary rainfall in a Dutch lowland catchment

C. C. Brauer¹, A. J. Teuling^{1,*}, A. Overeem^{1, **}, Y. van der Velde^{1,2}, P. Hazenberg¹, P. M. M. Warmerdam¹, and R. Uijlenhoet¹

¹Hydrology and Quantitative Water Management Group, Wageningen University, The Netherlands

²Soil Physics, Ecohydrology and Ground Water Management Group, Wageningen University, The Netherlands

* formerly at: Institute for Atmospheric and Climate Science, ETH Zurich, Switzerland

** now at: Royal Netherlands Meteorological Institute, De Bilt, The Netherlands

Received: 17 December 2010 – Accepted: 22 December 2010 – Published: 11 January 2011

Correspondence to: C. C. Brauer (claudia.brauer@wur.nl)

Published by Copernicus Publications on behalf of the European Geosciences Union.

[Title Page](#)

[Abstract](#)

[Introduction](#)

[Conclusions](#)

[References](#)

[Tables](#)

[Figures](#)

◀

▶

◀

▶

[Back](#)

[Close](#)

[Full Screen / Esc](#)

[Printer-friendly Version](#)

[Interactive Discussion](#)



Abstract

On 26 August 2010 the eastern part of The Netherlands and the bordering part of Germany were struck by a series of very heavy rainfall events lasting for more than a day. Over an area of 740 km^2 more than 120 mm of rainfall was observed in 24 h.

5 This extreme event resulted in local flooding of city centres, highways and agricultural fields, and considerable financial loss.

In this paper we report on the unprecedented flash flood triggered by this exceptionally heavy rainfall event in the 6.5 km^2 Hupsel Brook catchment, which has been the experimental watershed employed by Wageningen University since the 1960s. This 10 study aims to improve our understanding of the dynamics of such lowland flash floods. We present a detailed hydrometeorological analysis of this extreme event, focusing on its synoptic meteorological characteristics, its space-time rainfall dynamics as observed with rain gauges, weather radar and a microwave link, as well as the measured soil moisture, groundwater and discharge response of the catchment.

15 At the Hupsel Brook catchment 159.5 mm of rainfall was observed in 24 h, corresponding to an estimated return period in the order of 6000 years. As a result, discharge at the catchment outlet increased from 4.4 l s^{-1} to nearly $5 \text{ m}^3 \text{ s}^{-1}$ (i.e. a specific discharge of $0.77 \text{ m}^3 \text{ s}^{-1} \text{ km}^{-2}$, or 2.8 mm h^{-1}). Within 7 h discharge rose from 50 to $4.5 \text{ m}^3 \text{ s}^{-1}$.

20 The catchment response can be divided into four phases: (1) soil moisture reservoir filling, (2) groundwater response, (3) surface depression filling and surface runoff and (4) backwater feedback. The first 35 mm of rainfall were stored in the soil without a significant increase in discharge. Relatively dry initial conditions (in comparison to those for past discharge extremes) prevented an even faster and more vigorous hydrological 25 response.

Soil buffer limits flash flood response to extraordinary rainfall

C. C. Brauer et al.

[Title Page](#)

[Abstract](#)

[Introduction](#)

[Conclusions](#)

[References](#)

[Tables](#)

[Figures](#)

◀

▶

◀

▶

[Back](#)

[Close](#)

[Full Screen / Esc](#)

[Printer-friendly Version](#)

[Interactive Discussion](#)



Soil buffer limits flash flood response to extraordinary rainfall

C. C. Brauer et al.

Flash floods, defined here as extreme floods generated by intense precipitation over rapidly responding catchments, have recently drawn increased attention, both from the scientific community and from the media. Their often devastating consequences, both in terms of material damage and loss of life, have triggered a number of European research projects (e.g. FLOODsite, HYDRATE, and IMPRINTS) to study the meteorological causes and hydrological effects of such events. Examples of such studies are reported in the recent publications by Smith et al. (1996), Ogden et al. (2000), Gaume et al. (2003), Gaume et al. (2004), Delrieu et al. (2005) and Borga et al. (2007).

From the perspective of water management and early warning, one of the main challenges posed by the phenomenon of flash floods is the extremely rapid response times of many of the catchments involved (as short as 10 min for certain small urban watersheds in mountainous environments). The consequence of these short lead times is that hydrological forecasting systems for regions with catchments prone to flash floods must rely heavily on meteorological forecasts, either from radar-based short-term precipitation forecasting (nowcasting) or from numerical weather prediction. Improved forecasting and early warning of flash floods is crucial, because the extreme discharges associated with such events (maximum specific discharges can reach tens of $\text{m}^3 \text{ s}^{-1} \text{ km}^{-2}$) can have devastating societal consequences.

Typically, a timescale of a few hours is used to distinguish a flash flood from a regular flood. Since runoff generation is faster in mountainous catchments with steep slopes than in lowland catchments and since orography can impact the magnitude of rainfall extremes (Miglietta and Regano, 2008), most flash-floods occur in mountainous areas. However in case of extreme rainfall, rapid runoff generation due to overland flow can also trigger flash floods in lowland catchments (Van der Velde et al., 2010).

Lowland areas, such as the densely populated delta region of The Netherlands, are typically associated with large-scale flooding caused by rivers such as the Rhine and Meuse. These rivers have relatively slow response times (of the order of days

Title Page	
Abstract	Introduction
Conclusions	References
Tables	Figures
◀	▶
◀	▶
Back	Close
Full Screen / Esc	
Printer-friendly Version	
Interactive Discussion	



Soil buffer limits flash flood response to extraordinary rainfall

C. C. Brauer et al.

Title Page	
Abstract	Introduction
Conclusions	References
Tables	Figures
◀	▶
◀	▶
Back	Close
Full Screen / Esc	
Printer-friendly Version	
Interactive Discussion	

to weeks). However, heavy rainfall events and the associated local flooding do occur in The Netherlands (Monincx et al., 2006). In addition, the magnitude of 24-h rainfall extremes that can trigger such flooding is expected to increase in a warmer climate (Kew et al., 2010). Thus, an improved understanding of the hydrological processes involved in the response of both natural and man made (polder) catchments to local heavy rainfall is needed to support water management in lowland areas.

5

In this paper we report on the flash flood triggered by an exceptionally heavy rainfall event on 26 August 2010 that occurred exactly over the 6.5 km^2 Hupsel Brook catchment, which has been the experimental watershed employed by Wageningen University since the 1960s.

10

The catchment and used data will be described in Sect. 2. We present a detailed analysis of the synoptic meteorological situation leading to the event (Sect. 3.1), the rainfall accumulations as measured by rain gauges, weather radar, and a microwave link (Sects. 3.2 and 3.3) and the extreme value statistics of the rainfall accumulation (Sect. 3.4). The soil moisture, groundwater and surface water response within the catchment will be described in Sects. 4.1–4.3. We present a dissection of the observed hydrological response into a sequence of contrasting regimes that characterize the storage and discharge dynamics of the catchment following this extraordinary rainfall event (Sect. 5). Finally we present our conclusions (Sect. 6)

15

20

2 Hupsel Brook experimental catchment

2.1 Field site

25

The Hupsel Brook catchment is situated in the east of The Netherlands (Fig. 1). Its area is 6.5 km^2 , its elevation ranges from 22 to 35 m a.s.l. and the mean slope is 8% (Van der Velde et al., 2009). The brook itself is 4 km long and has 7 small tributaries with lengths varying from 300 to 1500 m (Warmerdam, 1979). The slope of the brook is about 2%. The land use is roughly 59% grassland, 33% agricultural (mostly maize), 3% forest and 5% built-on areas.

Soil buffer limits flash flood response to extraordinary rainfall

C. C. Brauer et al.

[Title Page](#)[Abstract](#)[Introduction](#)[Conclusions](#)[References](#)[Tables](#)[Figures](#)[◀](#)[▶](#)[◀](#)[▶](#)[Back](#)[Close](#)[Full Screen / Esc](#)[Printer-friendly Version](#)[Interactive Discussion](#)

The Hupsel Brook catchment was selected as a research catchment in the 1960s because of its hydrogeological setting. The top layer consists of loamy sand with some clay, peat and gravel layers. Its thickness increases from 0.2 m in the east to 10 m in the west. The sand layer is situated on an impermeable marine clay layer of more than 20 m thick. Consequently, there is one phreatic aquifer discharging to the brook and regional groundwater flow is assumed to be small.

The Hupsel Brook is natural, but both the catchment and the brook have been modified by human intervention (Warmerdam, 1979). The meandering brook has been straightened before the start of the observations (and parts are being restored since 2007). Several culverts have been constructed since the 1960s, which form potential obstacles during high flow conditions. Drainpipes are installed in about 50% of the plots to accommodate optimal groundwater levels for agriculture (Fig. 1) (Van der Velde et al., 2010). A dense network of ditches allows quick discharge when catchment storage is high, but the small (tertiary and secondary) ditches are often dry when catchment storage is low.

Since 1963 various hydrological, geological and meteorological measurement campaigns have been carried out, which have been well documented in the literature (e.g., Colenbrander, 1965; Stricker and Brutsaert, 1978; Stricker and Warmerdam, 1982; Hopmans and van Immerzeel, 1988; Van Ommen et al., 1989; Hopmans and Stricker, 1989; Puente et al., 1993; Van der Velde et al., 2009; Rozemeijer et al., 2010). We refer to these studies for more information on the catchment.

2.2 Data

The Royal Netherlands Meteorological Institute (KNMI) operates a network of 32 automated meteorological stations (with a density of about 1 station per 1000 km²), where among others 10-min values of rainfall (measured with an automatic rain gauge), global radiation and air temperature are collected. One of the meteorological stations is located within the Hupsel Brook catchment (Figs. 1 and 2).

Soil buffer limits flash flood response to extraordinary rainfall

C. C. Brauer et al.

[Title Page](#)[Abstract](#)[Introduction](#)[Conclusions](#)[References](#)[Tables](#)[Figures](#)[◀](#)[▶](#)[◀](#)[▶](#)[Back](#)[Close](#)[Full Screen / Esc](#)[Printer-friendly Version](#)[Interactive Discussion](#)

[Title Page](#)[Abstract](#)[Introduction](#)[Conclusions](#)[References](#)[Tables](#)[Figures](#)[◀](#)[▶](#)[◀](#)[▶](#)[Back](#)[Close](#)[Full Screen / Esc](#)[Printer-friendly Version](#)[Interactive Discussion](#)

and 27 August, 15:00 UTC) the gauge-adjusted 1-h radar rainfall depths at the same location have been used.

In a field (with drainpipes) located next to the meteorological station 31 piezometers have been installed (Fig. 1) (Van der Velde et al., 2009). This field slopes towards a ditch on one side of the field. The surface has local elevations and depressions with height differences of approximately 50 cm. Piezometers are situated both on local elevations and in local depressions to capture the differences in groundwater dynamics. In 14 of the 31 piezometers pressure sensors record water levels every 15 min. A number of Echoprobe capacitance sensors (type Echoprobe EC-20) were also installed in this field to measure soil moisture content. Here we use data from one sensor at 40 cm depth situated in a local elevation at 20 m from the ditch.

Since 1968, discharge data have been collected with a particular type of H-flume at the catchment outlet (Hooghart, 1984). Its temporal resolution for the period used in this paper was 15 min. Further details concerning the calibration of this flume are provided in Sect. 4.4.

2.3 Post-event field surveys

Post-event field surveys can provide valuable information on water levels and flow processes in ungauged parts of the catchment (Gaume, 2006; Gaume and Borga, 2008; Marchi et al., 2009). Such surveys were performed directly after the event on 27 August, as well as during several phases of the recession following the flash flood. During these surveys, photographs were taken on several locations in the catchment and all instrumentation was inspected. Additional information was provided by local inhabitants. A summary of the surveys is provided in Table 1.

2.4 Discharge regime

It is relevant to put the 27 August discharge peak, as well as the conditions prior to 26 August, into a historical perspective. Based on a time series of mean daily discharge

from 1969 to 2010 some statistics can be computed. Mean discharge at the outlet of the Hupsel Brook catchment is 60 l s^{-1} (0.8 mm d^{-1}). During 1% of the time 170 l s^{-1} is exceeded and during 1% of the time 924 l s^{-1} is exceeded.

The maximum discharge measured since 1969 was $3.0\text{ m}^3\text{ s}^{-1}$ and occurred on 5 December 1993. This discharge peak was caused by a rainfall event of 21 mm in one day and 38 mm of rainfall in the four preceding days. Since 1969, a daily mean discharge of $1\text{ m}^3\text{ s}^{-1}$ was exceeded five times. In Table 2 rainfall depths and durations, and initial and peak discharges are given for these events. Initial discharges (and most likely also initial storage) were much higher for the five previous discharge extremes 10 than on 26 August 2010, resulting in high discharges after much less rainfall.

Restricting the analysis to the conditions typical for the last decade of August (20–31 August), the mean discharge is 16 l s^{-1} and during 10% of the time 43 l s^{-1} is exceeded. Sometimes there is no or hardly any discharge. During 10% of the time 1.1 l s^{-1} is not reached. Before the start of this rainfall event, the discharge was 4.4 l s^{-1} , 15 a value that is exceeded 81% of the days and on 45% of the days in the last decade of August (Fig. 3). A discharge of 4.4 l s^{-1} is therefore low in terms of the mean for the end of August and also much lower than the initial conditions for the past extremes, but it is not exceptional.

3 Rainfall event

20 3.1 Synoptic situation and rainfall pattern

The synoptic chart at 26 August, 18:00 UTC shows an elongated region with multiple shallow low pressure centres stretching from the Bay of Biscay to Poland (Fig. 4). The low pressure centres were sandwiched between bands of high pressure over the north Atlantic and southern Europe, which allowed the system to be stationary during most 25 of the day. Because pressure gradients were small, wind speeds were low and storm cells moved slowly.

[Title Page](#)

[Abstract](#)

[Introduction](#)

[Conclusions](#)

[References](#)

[Tables](#)

[Figures](#)

◀

▶

◀

▶

[Back](#)

[Close](#)

[Full Screen / Esc](#)

[Printer-friendly Version](#)

[Interactive Discussion](#)



Soil buffer limits flash flood response to extraordinary rainfall

C. C. Brauer et al.

[Title Page](#)[Abstract](#)[Introduction](#)[Conclusions](#)[References](#)[Tables](#)[Figures](#)[◀](#)[▶](#)[◀](#)[▶](#)[Back](#)[Close](#)[Full Screen / Esc](#)[Printer-friendly Version](#)[Interactive Discussion](#)

Along these low pressure centres a warm front was present, which divided warm, humid air in the south from cooler air in the north. The temperature gradients over The Netherlands were large. For example, a difference of 8 °C in maximum daily surface temperature was found over 150 km.

5 The frontal transition zone of warm air in the south and cooler air in the north of The Netherlands caused several active disturbances during 26 August. In the course of the afternoon the atmosphere south of the warm front became unstable, giving rise to some very heavy, mostly convective rain showers in the middle and eastern part of the country. These disturbances were part of a mesoscale convective system and 10 passed The Netherlands with a west-southwesterly flow, locally resulting in extraordinary accumulations of rainfall (see Schumacher and Johnson, 2005, for a description of a mesoscale convective system). Similar accumulations were recorded in parts of Northwestern Germany (Fig. 4).

15 Because storm cells moved along a stationary line, it rained continuously for long periods of time in several places. More than 18 h of continuous rainfall was recorded in De Bilt (the location of the used KNMI weather radar).

20 The rainfall pattern which lead to these heavy intensities was highly variable, containing both convective and stratiform rainfall. Figure 5 presents a clear example of the spatial variability in the rainfall field as observed by the weather radar in De Bilt at 19:15 UTC. This weather radar scans at different angles, which makes it possible to obtain a vertical profile of radar reflectivity (Hazenberg et al., 2010). In Fig. 5 both the horizontal and vertical extent of the convective area (reflectivity exceeding 40 dBZ) can be clearly identified.

25 The convective cells were part of a larger southwest-northeast oriented squall line that became apparent in the Hupsel Brook catchment at 15:30 UTC (see also Fig. 6). In this squall line new convective cells with heavy precipitation were generated upstream of the Hupsel Brook catchment until 22:15:00 UTC. This happens often in mesoscale convective systems and can lead to extreme rainfall accumulations (Schumacher and Johnson, 2008). The convective areas were highly variable in space, but many passed

over the Hupsel Brook catchment. After 22:15 UTC rainfall got a more stratiform character.

3.2 Estimation using rain gauges and weather radar

Figure 2 shows daily rainfall depths for 26 August, 08:00 UTC to 27 August, 08:00 UTC for the gauge-adjusted radar composite and the interpolated manual rain gauge data. Locations of the manual rain gauges and their observed daily sums are also shown.

The highest manual rain gauge rainfall depth for this day (138.2 mm) was observed in Lielvelde, 4 km southwest of the catchment. This, for Dutch conditions, extraordinary accumulation belongs to the highest ever recorded in The Netherlands since official registration of the national rain gauge network started in 1951. The highest daily rainfall depth measured (with manual rain gauges) since 1951 was 148 mm, the second highest 146 mm (source: KNMI). The 3rd, 5th and 7th places are occupied by Lielvelde (138.2 mm), Hupsel (130.5 mm) and Rekken (125.9 mm), all from 26 August, 08:00 UTC to 27 August, 08:00 UTC (all plotted in Fig. 2). A less official record from the KNMI shows another maximum: on 3 August 1948, 208 mm of rainfall was measured.

At the location of the automatic rain gauge in the catchment a gauge-adjusted radar rainfall depth of 140.7 mm was measured (08:00–08:00 UTC). Based on the data series from the automatic rain gauge (gaps filled with radar data), the maximum daily (08:00–08:00 UTC) rainfall depth is 146.3 mm and the maximum 24-h rainfall depth is 159.5 mm (04:00–04:00 UTC). This is larger than the largest 24-h rainfall depth observed in the 11-year climatological radar data set for the entire land surface of The Netherlands (142 mm for a radar pixel of 6 km^2).

Figure 6 shows that the cumulative rainfall depths from 26 August, 08:00 UTC to 26 August, 21:00 UTC from the automatic rain gauge and the gauge-adjusted radar hardly differ. Daily accumulations from radar and manual rain gauge are comparable, which is partly induced by the gauge-adjustment of the radar data. Temporal rainfall variations from radar and rain gauge (not induced by daily gauge-adjustment) are quite similar as well.

Title Page	
Abstract	Introduction
Conclusions	References
Tables	Figures
◀	▶
◀	▶
Back	Close
Full Screen / Esc	
Printer-friendly Version	
Interactive Discussion	

Soil buffer limits flash flood response to extraordinary rainfall

C. C. Brauer et al.

[Title Page](#)[Abstract](#)[Introduction](#)[Conclusions](#)[References](#)[Tables](#)[Figures](#)[◀](#)[▶](#)[◀](#)[▶](#)[Back](#)[Close](#)[Full Screen / Esc](#)[Printer-friendly Version](#)[Interactive Discussion](#)

The rainfall event can be divided into roughly four parts according to rainfall intensity (see also Figs. 6 and 9). From 04:00 to 10:00 UTC rainfall was moderately intense (27.2 mm; mean rainfall intensity 4.5 mm h^{-1}), from 10:00 to 15:00 UTC rainfall was light (4.7 mm; mean rainfall intensity 0.9 mm h^{-1}), from 15:00 to 22:00 UTC rainfall was intense (111.0 mm; mean rainfall intensity 15.9 mm h^{-1}) and from 22 to 03:00 UTC rainfall was moderately intense (16.3 mm; mean rainfall intensity 3.3 mm h^{-1}).

From the gauge-adjusted radar composite the spatial extent (including a part of Germany) of the extreme event is derived for the largest 24-h rainfall depths (04:00–04:00 UTC). The 24-h rainfall depth exceeds 100 mm for a 2100 km^2 area, 120 mm for a 740 km^2 area, and 140 mm for a 170 km^2 area. The scale of this event is considerably larger than the largest scale of the 24-h rainfall depth exceeding 100 mm, $\sim 450 \text{ km}^2$, as found in the 11-year climatological radar data set for The Netherlands (Overeem et al., 2010a).

3.3 Estimation using microwave link

15 Microwave links can potentially be used to provide rainfall estimates in data-sparse regions or during extreme events.

During the event of 26 August, the microwave link connection remained stable up to a radar rainfall depth of 80 mm and the obtained depths correspond well to the radar depths measured over the same path (Fig. 6). Figure 7 shows that the dynamics 20 of the link-based rainfall intensities are similar to those obtained from path-averaged gauge-adjusted radar rainfall intensities. This confirms that microwave links are a useful addition to the existing networks and that they can be used to estimate rainfall in areas where no gauges are available.

This is a simple, first-order attempt to estimate rainfall intensities from this commercial microwave link: Some important sources of error were not taken into account: (1) there may be attenuation due to wet antennas, (2) mean rainfall intensities are simply calculated as the average of the minimum and maximum rainfall intensities, and (3) the 25 large spatial rainfall variability, as indicated by Figs. 2 and 5, can cause overestimation

for a link of this frequency (15.3 GHz). both instantaneously (Fig. 5) and accumulated over the entire event (Fig. 2) can cause systematic deviations (Overeem et al., 2010b).

3.4 Estimation of return period

While the rainfall event can easily be characterized as extraordinary based on the analysis in Sect. 3.2, the question remains how extreme this event really was, and what the probability is of such an event happening again in the near future. Figure 8 shows a probability plot of 24-h rainfall depths, based on Overeem et al. (2008), who performed an extreme value analysis of rainfall depths from time series of 12 automatic rain gauges in The Netherlands (altogether 514 years of data). A rough estimate of the average return period of the 24-h rainfall depth for this event (based on automatic rain gauge and radar data), 159.5 mm (red square), is in the order of 6000 years for a given location.

When the extreme value analysis is repeated including the 159.5 mm rainfall depth, the average return period decreases to the order of 3000 years. Note that this hardly influences the quantiles of rainfall depths for average return periods up to about 100 years. Of course, these return periods are significantly longer than the return period of 159.5 mm being exceeded in 24 h at an arbitrary location in The Netherlands.

The uncertainties due to sampling variability have been shown to be large (Overeem et al., 2008). Using the bootstrap method the 95% confidence interval was obtained. For the 24-h accumulation for a return period of 6000 years this interval ranges from 129 to 199 mm. Despite this large uncertainty, it is clear from Fig. 8 that the return period is well above 1000 years. The probability of such an event occurring at our experimental catchment between the start of the measurements in the 1960s and now is estimated to be less than 2%.

[Title Page](#)

[Abstract](#)

[Introduction](#)

[Conclusions](#)

[References](#)

[Tables](#)

[Figures](#)

◀

▶

◀

▶

[Back](#)

[Close](#)

[Full Screen / Esc](#)

[Printer-friendly Version](#)

[Interactive Discussion](#)



4.1 Soil moisture response

When rainfall infiltrates into the unsaturated zone, soil moisture can be expected to react before groundwater and runoff. Figure 9 shows the observed local response of soil moisture content. Before the rainfall event, the soil was relatively dry. The soil moisture content measured by the available sensor at 40 cm depth was initially 23% and started to rise at 07:00 UTC, 3 h after the start of the rainfall event. As a result of the first part of the rainfall event with moderate intensities (04:00–09:00 UTC) the soil moisture content rose slowly to 32% at 10:00 UTC. Between 09:00 and 10:00 UTC 12 mm of rainfall was registered, leading to a steep increase in soil moisture content up to 41% at 11:00 UTC. Between 10:00 and 12:00 UTC there was hardly any rainfall and the soil moisture content remained constant, but between 12:00 and 13:00 UTC another 3.6 mm of rainfall occurred and the soil moisture content reached saturation (45%) at 14:30 UTC. After that, the soil moisture content slowly decreased, but remained above 40% until 27 August, 19:30 UTC. The high soil moisture contents contributed to the strong groundwater table response. It should be noted that soil moisture contents returned to pre-event levels within 3 days.

4.2 Groundwater response

The depth and dynamics of the groundwater levels depend on the distance to the ditch and on the microtopography (Van der Velde et al., 2010). In Fig. 9 groundwater depths are shown for 2 of the 14 recorded piezometers; one located in a local depression and one on a local elevation.

Initially, groundwater depths measured by two piezometers shown in Fig. 9 were 90 and 115 cm below surface. It took until 11:30 UTC before groundwater levels slowly started to rise, more than 4.5 h after the initial increase in soil moisture content was observed. In the groundwater time series, the influence of single peaks in rainfall

Title Page	
Abstract	Introduction
Conclusions	References
Tables	Figures
◀	▶
◀	▶
Back	Close
Full Screen / Esc	
Printer-friendly Version	
Interactive Discussion	



intensity is not visible. At 17:30 UTC, when groundwater levels were 48 and 88 cm below surface, groundwater rise accelerated. This was 7.5 h after the soil moisture content increase accelerated. Groundwater rise accelerated when soil moisture content increased, because less water could be stored in the unsaturated zone. In addition, 5 rainfall intensity increased after 15:00 UTC and therefore more water was available to fill the pore spaces.

Around 20:15 UTC, the soil at the local depression became completely saturated and 10 ponding occurred. Due to the larger available storage, it took until 22:45 UTC for the soil at the local elevation to become completely saturated. Ponding was less pronounced here likely due to water flowing into the local depressions. Because ponding did not 15 occur, the groundwater level at the local elevations showed strong dynamics during and after rainfall events, while the groundwater level in the local depression remained above land surface for 6 days, with a maximum ponding depth of 11 cm. Similar ponding depths were also observed in the field during post-event field survey II, with many of the local depressions still filled.

During post-event field survey II water was still flowing overland from the ponds in the fields to the ditches at several places. Overland flow is usually assumed to be of little importance in relatively flat areas, but can occur in lowland areas such as The Netherlands in case of high groundwater tables and/or high rainfall intensities (Appels 20 et al., 2010). During post-event field survey II some farmers were seen digging small channels in the field to reduce ponding and transport the water to the ditches more quickly.

Uncertainty in interpreting these measurements arises mostly from sampling variability. Both soil moisture and groundwater depth are highly variable in space. Therefore, 25 these measurements do not provide the catchment representative soil moisture content or groundwater depth, but provide a mere indication of their dynamics.

[Title Page](#)

[Abstract](#)

[Introduction](#)

[Conclusions](#)

[References](#)

[Tables](#)

[Figures](#)

◀

▶

◀

▶

[Back](#)

[Close](#)

[Full Screen / Esc](#)

[Printer-friendly Version](#)

[Interactive Discussion](#)



4.3 Discharge response

Discharge showed little to no response to the first 35 mm of rainfall which were absorbed in the soil. Discharge started to rise slowly 7 h after the start of the rainfall event. Within 23 h, from 26 August 04:15 UTC to 27 August 02:45 UTC, discharge increased from 4.4 l s^{-1} to the maximum observed value of $4.98 \text{ m}^3 \text{ s}^{-1}$, i.e., by more than three orders of magnitude. The discharge increased from 50 l s to $4.5 \text{ m}^3 \text{ s}^{-1}$ in 7 h. The most spectacular rise took place on 26 August between 17:30 and 22:30 UTC, when discharge increased from $0.42 \text{ m}^3 \text{ s}^{-1}$ to $4.0 \text{ m}^3 \text{ s}^{-1}$.

Discharge remained above $1 \text{ m}^3 \text{ s}^{-1}$ for 28 h and exceeded the 99% percentile (455 l s^{-1}) for 4 days (Fig. 3). In Fig. 9e it seems that discharge drops to its pre-event level within days, but on logarithmic scale (Fig. 9d) it can be seen that this would take weeks. On 3 September (at the end of the period shown in Fig. 9) discharge was still 150 l s^{-1} ; a value which is exceeded only 10% of the time.

Between 26 August and 7 September, 184 mm of rainfall was recorded (by the automatic rain gauge, with data gaps filled with gauge-adjusted radar data). In the same period 92 mm was discharged, yielding a runoff ratio of 50%. The other 50% has been stored in the soil ($\sim 70 \text{ mm}$) or has evaporated (20–25 mm).

There are some constructions in or around the brook that become obstacles in case of high discharges. The most important structures influencing the flow regime are the culverts. When discharge exceeds the design discharge of the culverts, the excess water is stored upstream of the culvert in the brook or on the floodplain. Just 100 m upstream of the catchment outlet is a culvert with a maximum capacity of about $5 \text{ m}^3 \text{ s}^{-1}$, which likely topped off the discharge peak at the flume at about $5 \text{ m}^3 \text{ s}^{-1}$.

When catchment storage increases, the dense network of drainpipes and ditches becomes more important. Before the rainfall event, groundwater levels were below the level of drainpipes, tertiary ditches and most of the secondary ditches. The drainage network was therefore not fully used and transport of water was mostly through the subsurface and slow. When groundwater levels rose, drainpipes and ditches started

Title Page	
Abstract	Introduction
Conclusions	References
Tables	Figures
◀	▶
◀	▶
Back	Close
Full Screen / Esc	
Printer-friendly Version	
Interactive Discussion	



to transport water, leading to an increase in discharge capacity and in discharge itself. Without this drainage network, ponding depths and the resulting damage would have been larger in the Hupsel Brook catchment.

The peak of $4.98 \text{ m}^3 \text{ s}^{-1}$ corresponds to a specific discharge of $0.77 \text{ m}^3 \text{ s}^{-1} \text{ km}^{-2}$, or 2.8 mm h^{-1} , which is exceptional for a small catchment with an average slope of only 8%. The limited number of years for which discharge data are available, however, prevent an accurate estimation of the return period of this peak discharge. It seems likely, however, that the return period for the discharge peak is (much) less extreme than the return period for the 24-h rainfall accumulation due to the buffering effect of the unsaturated zone.

4.4 Discharge accuracy

The flume at the catchment outlet is situated in a dam perpendicular to the brook with a higher level than the rim of the flume (Fig. 9). In post-event field surveys no evidence was found that water had flown over the dam. Hence all water must have passed over the flume.

It is not likely that water levels in the flume have risen higher than the measuring range of the stilling well. The maximum water height measured in the flume was 1.504 m, 4 mm higher than the rim, leading to a computed peak discharge of $4.98 \text{ m}^3 \text{ s}^{-1}$.

Because the flume is slightly narrower than a standard H-flume, the flume was calibrated in the Wageningen University hydraulics laboratory in 1969 and 1983 (Fig. 10). For low discharges a prototype was used and for high discharges a scale model. The flume was calibrated up to a water level of 1.22 m and corresponding discharge of $3.02 \text{ m}^3 \text{ s}^{-1}$. The obtained stage-discharge relationship was extrapolated to the maximum water level of 1.5 m, resulting in a discharge of $4.94 \text{ m}^3 \text{ s}^{-1}$.

To examine if such an extrapolation is valid, we compared laboratory experiments from our flume to those of standard H- and HL-flumes, which have been calibrated to the rim (Kilpatrick and Schneider, 1983). For each flume, water levels and discharges

[Title Page](#)

[Abstract](#)

[Introduction](#)

[Conclusions](#)

[References](#)

[Tables](#)

[Figures](#)

[◀](#)

[▶](#)

[◀](#)

[▶](#)

[Back](#)

[Close](#)

[Full Screen / Esc](#)

[Printer-friendly Version](#)

[Interactive Discussion](#)



are normalized with respect to their maximum values and plotted against each other (Fig. 10). The deviations between the stage-discharge relationships of the different types of H-flumes were very small, from which we conclude that the employed extrapolation does not introduce significant errors.

5 During post-event field survey I (13 h after the peak), the flume was found to be partially submerged (i.e., the water level downstream of the flume was higher than the crest of the flume). When flumes are submerged, water downstream of the flume introduces an additional resistance, leading to higher stage heights in the flume at a given discharge. When measured stage heights are used to compute discharges 10 without accounting for (partial) submergence, the discharge will be overestimated.

15 Fortunately, H-flumes are not sensitive to submergence. When the submergence ratio (water level downstream of the flume divided by stage height, both with respect to the crest) of a standard H-flume is 50%, the stage height is overestimated by only 3% (Brakensiek et al., 1979). A submergence ratio of 60% leads to a stage height 20 overestimation of 5%. These values may differ slightly for the Hupsel flume. During post-event field survey I, the submergence ratio was estimated to be 56% ($h_{\text{upstream}} = 1.23 \text{ m}$ and $h_{\text{downstream}} = 0.7 \text{ m}$). This leads to an overestimation of the stage height by 4% (based on data for H-flumes) and a possible overestimation of the discharge by 10% ($3.07 \text{ m}^3 \text{ s}^{-1}$ as an initial estimate and $2.80 \text{ m}^3 \text{ s}^{-1}$ after correction). During the peak, this effect might even have been smaller. Since we lack detailed information on downstream water levels, we assume that possible errors due to submergence are small enough to be neglected.

5 Synthesis of the hydrologic response

25 In many catchments, a close relation exists between the discharge at the outlet and the total amount of mobile water stored in the catchment (e.g., Kirchner, 2009; Teuling et al., 2010). While storage cannot be measured directly at the catchment scale, storage changes can be calculated by using the water balance over periods during which

[Title Page](#)

[Abstract](#)

[Introduction](#)

[Conclusions](#)

[References](#)

[Tables](#)

[Figures](#)

◀

▶

◀

▶

[Back](#)

[Close](#)

[Full Screen / Esc](#)

[Printer-friendly Version](#)

[Interactive Discussion](#)



all fluxes are known. In case of the Hupsel flash flood, the contribution of evapotranspiration to the water balance is negligible around the discharge peak. Rainfall measured at the meteorological station may be considered representative for the whole 6.5 km² catchment. Hence, storage S can be calculated with respect to an arbitrary reference

5 level S_0 by integrating the difference between rainfall R and discharge Q over time t :

$$S = S_0 + \int_{t=t_0}^t (R - Q) dt. \quad (1)$$

In Fig. 11 both discharge and groundwater levels are plotted against total catchment storage as calculated by Eq. (1) for the period between 25 August 18:00 UTC and 27 August 18:00 UTC.

10 When interpreting the lines in Fig. 11 it should be noted that water can be stored in the catchment in different ways: (1) as soil moisture in the unsaturated zone, (2) as groundwater in the saturated zone, (3) as ponds in local depressions on the fields or (4) as surface water in the brook or on banks and land surface in the floodplain. The subsequent filling of these stores, along with the interaction between them, ultimately 15 determines the catchment response during the onset and peak of the flood. We hypothesize that the discharge dynamics at the catchment outlet reflect the following stages, each of which has a different sensitivity of discharge to storage changes:

(1) *Soil moisture reservoir filling* – initially the upper part of the soil is dry, and rainfall 20 is readily absorbed in the unsaturated zone. This leads to an increase in soil moisture content, but a lack of conductivity prevents groundwater levels to rise in conjunction with soil moisture. As a result, the discharge during this phase is hardly sensitive to storage changes up to a storage increase of ~30 mm.

(2) *Groundwater response* – the unsaturated zone is near saturation and additional rainfall readily leads to saturation of the soil matrix. Under these conditions the specific 25 yield μ is very small (0.06 over a large part of the storage increase in Fig. 11) and hydraulic heads can rise rapidly. Since groundwater levels strongly control the field-scale subsurface flow to the network of secondary and tertiary ditches, the discharge

is moderately sensitive to changes in total catchment storage. The rapid rise of groundwater levels continues up to a storage increase of $\sim 120\text{--}130\text{ mm}$, when groundwater levels reach the surface and ponding occurs.

(3) *Surface depression filling and surface runoff* – when ponding occurs, two mechanisms come into play with contrasting effects on the discharge increase. First, the specific yield strongly increases (since for ponded areas $\mu=1$), effectively reducing the increase in hydraulic heads in response to rainfall. Secondly, however, when ponds start to connect to the network of ditches, overland flow becomes an important runoff mechanism and discharge increases rapidly. This is a typical mechanism during flash floods and the moment at which overland flow is initiated determines for a large part the timing of flash flood response (Marchi et al., 2010). This is also the case in the Hupsel Brook catchment. The slope of the line in Fig. 11a is very steep between total catchment storage of 120 mm and 135 mm. Measured groundwater levels indicate phreatic surfaces extending to above the local height of the land surface (which was confirmed by observations during post-event field surveys).

(4) *Backwater feedback* – in the fourth phase discharge increases to above the design discharge of the culverts, leading to backwater feedbacks and extensive flooding of fields upstream of the culverts (Fig. 12). Such flooding was observed during post-event field surveys I and II (Fig. 9), especially in the area with elevation below 26 m (Fig. 1). The backwater effects strongly reduce the local pressure gradients that drive the flow of water through the subsurface. At the same time, they flatten the discharge peak. Figure 11 shows that high discharge levels persist during the decrease of the initial 20 mm of storage – consistent with the role of backwater.

Because initial groundwater levels, initial soil moisture contents, hydrogeology and land use vary spatially over the catchment, the timing of the different phases also varies spatially. During post-event field survey II more flooding was visible in the south-eastern part of the catchment, where the aquifer is thinner and groundwater levels shallower than in the western part. Therefore these phases cannot be separated exactly in Fig. 11. Nevertheless, these four stages appear to describe the observed

Soil buffer limits flash flood response to extraordinary rainfall

C. C. Brauer et al.

[Title Page](#)

[Abstract](#)

[Introduction](#)

[Conclusions](#)

[References](#)

[Tables](#)

[Figures](#)

◀

▶

◀

▶

[Back](#)

[Close](#)

[Full Screen / Esc](#)

[Printer-friendly Version](#)

[Interactive Discussion](#)



hydrological response of the Hupsel Brook catchment to the extraordinary rainfall of 26 August 2010 well.

The stages resemble the stages identified by Maréchal et al. (2009), who described a flash flood response in a karstic area. Here, a first rainfall event only caused soil saturation but a second caused a flash-flood due to overland flow. In addition, Maréchal et al. (2009) reported on backwater feedbacks at locations with limited discharge capacity.

We believe that because of the rapid increase in runoff during stage 3, in combination with the extremity of the rainfall, the magnitude of the discharge peak, the local flooding and widespread surface runoff, this runoff event is best characterized as a lowland flash flood.

6 Conclusions

On 26 August 2010 the eastern part of The Netherlands was struck by a series of very heavy rainfall events lasting for more than a day. These events lead to extraordinary 24-h rainfall accumulations (locally exceeding 150 mm) and unprecedented peak discharges.

Rainfall was measured in the Hupsel Brook catchment with rain gauges (one automatic and one manual), a weather radar and a microwave link. The maximum 24-h rainfall depth was 159.5 mm (measured with the automatic rain gauge, of which gaps were filled with gauge-adjusted radar data). This rainfall depth corresponds to an estimated return period of the order of 6000 years. The temporal dynamics and accumulations of rainfall intensities measured by the microwave link compare well to those of gauge-adjusted radar rainfall intensities averaged over the path of the microwave link. However, some important sources of error were not taken into account.

This rainfall event lead to a catchment response that is best described as a lowland flash flood, because of the extremity of the rainfall and the widespread surface runoff. Discharge at the catchment outlet increased from 4.4 l s^{-1} to nearly $5 \text{ m}^3 \text{ s}^{-1}$

[Title Page](#)

[Abstract](#)

[Introduction](#)

[Conclusions](#)

[References](#)

[Tables](#)

[Figures](#)

[◀](#)

[▶](#)

[◀](#)

[▶](#)

[Back](#)

[Close](#)

[Full Screen / Esc](#)

[Printer-friendly Version](#)

[Interactive Discussion](#)



(i.e. a specific discharge of $0.77 \text{ m}^3 \text{ s}^{-1} \text{ km}^{-2}$, or 2.8 mm h^{-1}). Although this event was extreme, a detailed analysis has revealed that discharge has been measured relatively accurately.

The catchment response can be divided in four phases: (1) *Soil moisture reservoir filling* – water is used to replenish soil moisture and discharge hardly rises. (2) *Groundwater response* – groundwater levels rise and discharge rises slowly. (3) *Surface depression filling and surface runoff* – ponds form in local depressions on the land surface, leading to surface runoff and rapid rise of discharge. (4) *Backwater feedback* – brook discharges exceed maximum discharge capacity of culverts in the brook. Water is stored behind the culverts, discharge does not increase anymore and local gradients that drive subsurface flow are reduced.

During this extreme event some thresholds became apparent that do not play a role during average conditions. Culverts do not influence the rainfall-runoff characteristics much in average situations, but become an important threshold in case of high discharges, when discharges are topped off, surface water levels rise and groundwater gradients are reduced. Often rainfall-runoff models are designed and calibrated with less extreme discharge data and then used to forecast peak flows. In these models, thresholds are not taken into account and as a consequence peak discharges are over-estimated. Incorporation of such thresholds in hydrological models is currently being performed and shall be reported in future work.

Low initial catchment storage acted as a soil buffer and likely reduced the magnitude of the hydrologic response. The first 35 mm of rainfall were stored in the soil without a significant increase in discharge. Only after 35 mm of rainfall, discharge started to rise more rapidly, leading to a lowland flash flood with an unprecedented peak discharge.

Acknowledgements. We thank Annemarie Braam (KNMI) for providing us an internal report of the Weather Service department, which has been used in the description of the synoptic situation. We acknowledge the E-OBS dataset from the EU-FP6 project ENSEMBLES (<http://ensembles-eu.metoffice.com>) and the data providers in the ECA&D project (<http://eca.knmi.nl>). We thank KNMI for providing the radar and rain gauge data, T-Mobile Netherlands for the



microwave link data, Deltas for groundwater and soil moisture data, Gert van den Houten (Water Board Rijn and IJssel) for the discharge data, ECMWF for ERA Interim data and Anton Dommerholt for the calibration data of the flume. We thank Jacqueline Meerink for providing photographs of the local flooding on 27 August, which helped us to assess the hydrologic response. A. J. Teuling acknowledges financial support from The Netherlands Organisation for Scientific Research through Veni Grant 016.111.002. P. Hazenberg and R. Uijlenhoet are financially supported by the EU-project IMPRINTS (FP7-ENV-2008-1-226555).

References

Appels, W., Bogaart, P., and van der Zee, S.: Influence of spatial variations of microtopography and infiltration on surface runoff and field scale hydrological connectivity, *Adv. Water Resour.*, in press, 2010. 124

Borga, M., Boscolo, P., Zanon, F., and Sangati, M.: Hydrometeorological analysis of the 29 August 2003 flash flood in the Eastern Italian Alps, *J. Hydrometeorol.*, 8, 1049–1067, 2007. 113

Brakensiek, D., Osborn, H., and Rawls, W.: Field manual for research in agricultural hydrology, vol. 224 of Agricultural Handbook, US Department of Agriculture, 1979. 127

Colenbrander, H.: The research watershed “Leerinkbeek” Netherland, in: IAHS Redbooks, vol. 66-II, pp. 558–563, 1965. 115

Delrieu, G., Ducrocq, V., Gaume, E., Nicol, J., Payrastre, O., Yates, E., Kirstetter, P.-E., Andrieu, H., Ayral, P.-A., Bouvier, C., Creutin, J.-D., Livet, M., Anquetin, S., Lang, M., Neppel, L., Obled, C., Parent-du-Châtelet, J., Saulnier, G.-M., Walpersdorf, A., and Wobrock, W.: The catastrophic flash-flood event of 8–9 September 2002 in the Gard region, France: a first case study for the Cévennes-Vivarais Mediterranean Hydrometeorological Observatory, *J. Hydrometeorol.*, 6, 34–52, 2005. 113

Gaume, E.: Post Flash-flood Investigations – Methodological Note, FLOODsite Report T23-06-0, 2006. 117

Gaume, E. and Borga, M.: Post-flood field investigations in upland catchments after major flash floods: proposal of a methodology and illustrations, *Journal of Flood Risk Management*, 1, 175–189, 2008. 117

Gaume, E., Livet, M., and Desbordes, M.: Study of the hydrological processes during the Avène River extraordinary flood (south of France): 6–7 October 1997, *Phys. Chem. Earth*, 28, 263–267, 2003. 113

[Title Page](#)

[Abstract](#)

[Introduction](#)

[Conclusions](#)

[References](#)

[Tables](#)

[Figures](#)

◀

▶

◀

▶

[Back](#)

[Close](#)

[Full Screen / Esc](#)

[Printer-friendly Version](#)

[Interactive Discussion](#)



Soil buffer limits flash flood response to extraordinary rainfall

C. C. Brauer et al.

Gaume, E., Livet, M., Desbordes, M., and Villeneuve, J. P.: Hydrological analysis of the river Aude, France, flash flood on 12 and 13 November 1999, *J. Hydrol.*, 286, 135–154, 2004. 113

5 Haylock, M., Hofstra, N., Klein Tank, A., Klok, E., Jones, P., and New, M.: A European daily high-resolution gridded dataset of surface temperature and precipitation, *J. Geophys. Res.-Atmos.*, 113, D20119, 2008. 141

Hazenberg, P., Leijnse, H., and Uijlenhoet, R.: Radar rainfall estimation of stratiform winter precipitation in the Belgian Ardennes, *Water Resour. Res.*, in press, 2010. 119

10 Hooghart, J.: Vergelijking van modellen voor het onverzadigd grondwatersysteem en de ver-damping. Verslag van de 4e CHO-studiebijeenkomst in samenwerking met de Studiegroep Hupselse Beek, Tech. Rep. 13, Commissie voor Hydrologisch Onderzoek TNO, in Dutch, 1984. 117

Hopmans, J. and van Immerzeel, C.: Variation in evapotranspiration and capillary rise with changing soil profile characteristics, *Agr. Water Manage.*, 13, 295–305, 1988. 115

15 Hopmans, J. W. and Stricker, J. N. M.: Stochastic analysis of soil water regime in a watershed, *J. Hydrol.*, 105, 57–84, 1989. 115

Hosking, J. and Wallis, J.: *Regional Frequency Analysis: an Approach Based on L-moments*, Cambridge University Press, Cambridge, 1997. 145

20 Kew, S. F., Selten, F. M., Lenderink, G., and Hazeleger, W.: Robust assessment of future changes in extreme precipitation over the Rhine basin using a GCM, *Hydrol. Earth Syst. Sci. Discuss.*, 7, 9043–9066, doi:10.5194/hessd-7-9043-2010, 2010. 114

Kilpatrick, F. and Schneider, V.: Use of flumes in measuring discharge, vol. 3 of US Geological Survey Techniques of Water-Resources Investigations, chap. A14, US Department of the Interior, 1983. 126, 148

25 Kirchner, J.: Catchments as simple dynamical systems: catchment characterization, rainfall – runoff modeling, and doing hydrology backwards, *Water Resour. Res.*, 45, W02429, doi:10.1029/2008WR006912, 2009. 127

Leijnse, H., Uijlenhoet, R., and Stricker, J. N. M.: Rainfall measurement using radio links from cellular communication networks, *Water Resour. Res.*, 43, W03201, 2007. 116

30 Marchi, L., Borga, M., Preciso, E., Sangati, M., Gaume, E., Bain, V., Delrieu, G., Bonnifait, L., and Pogačnik, N.: Comprehensive post-event survey of a flash flood in Western Slovenia: observation strategy and lessons learned, *Hydrol. Process.*, 23, 3761–3770, 2009. 117

Marchi, L., Boraga, M., Preciso, E., and Gaume, E.: Characterisation of selected extreme flash

Discussion Paper | Discussion Paper

Title Page	
Abstract	Introduction
Conclusions	References
Tables	Figures
◀	▶
◀	▶
Back	Close
Full Screen / Esc	
Printer-friendly Version	
Interactive Discussion	



Soil buffer limits flash flood response to extraordinary rainfall

C. C. Brauer et al.

[Title Page](#)[Abstract](#)[Introduction](#)[Conclusions](#)[References](#)[Tables](#)[Figures](#)[◀](#)[▶](#)[◀](#)[▶](#)[Back](#)[Close](#)[Full Screen / Esc](#)[Printer-friendly Version](#)[Interactive Discussion](#)

water quality, *Environ. Pollut.*, 158, 3571–3579, 2010. 115

5 Schumacher, R. and Johnson, R.: Organization and environmental properties of extreme-rain-producing mesoscale convective systems, *Mon. Weather Rev.*, 133, 961–976, 2005. 119

Schumacher, R. and Johnson, R.: Mesoscale processes contributing to extreme rainfall in a midlatitude warm-season flash flood, *Mon. Weather Rev.*, 136, 3964–3986, 2008. 119

10 Smith, J. A., Baeck, M. L., Steiner, M., and Miller, A. J.: Catastrophic rainfall from an up-slope thunderstorm in the central Appalachians: the Rapidan storm of June 27, 1995, *Water Resour. Res.*, 32, 3099–3113, 1996. 113

Stricker, J. and Brutsaert, W.: Actual evapotranspiration over a summer in the Hupsel Catchment, *J. Hydrol.*, 39, 139–157, 1978. 115

15 Stricker, J. N. M. and Warmerdam, P. M. M.: Estimation of the water balance in the Hupselse Beek basin over a period of three years and a first effort to simulate the rainfall-runoff process for a complete year, in: *Proceedings of the International Symposium on Hydrological Research Basins and Their Use in Water Resources Planning*, 79–388, Bern, Switzerland, 1982. 115

Teuling, A. J., Lehner, I., Kirchner, J. W., and Seneviratne, S. I.: Catchments ad simple dynamical systems: Experience from a Swiss prealpine catchment, *Water Resour. Res.*, 46, W10502, 2010. 127

20 van der Velde, Y., de Rooij, G. H., and Torfs, P. J. J. F.: Catchment-scale non-linear groundwater-surface water interactions in densely drained lowland catchments, *Hydrol. Earth Syst. Sci.*, 13, 1867–1885, doi:10.5194/hess-13-1867-2009, 2009. 114, 115, 117

Van der Velde, Y., Rozemeijer, J., de Rooij, G., van Geer, F., and Broers, H.: Field scale measurements for separation of catchment discharge into flow route contributions, *Vadose Zone J.*, 9, 25–35, 2010. 113, 115, 123, 138

25 Van Ommen, H., Dijksma, R., Hendrickx, J., Dekker, L., Hulshof, J., and van den Heuvel, M.: Experimental assessment of preferential flow paths in a field soil, *J. Hydrol.*, 105, 253–262, 1989. 115

Warmerdam, P.: Hydrological effects of drainage improvement in the Hupselse Beek catchment area in the Netherlands, Tech. Rep. 64, Department of Hydraulics and Catchment Hydrology, Agricultural University, Wageningen, The Netherlands, 1979. 114

30 Younis, J., Anquetin, S., and Thielen, J.: The benefit of high-resolution operational weather forecasts for flash flood warning, *Hydrol. Earth Syst. Sci.*, 12, 1039–1051, doi:10.5194/hess-12-1039-2008, 2008. 116

Soil buffer limits flash flood response to extraordinary rainfall

C. C. Brauer et al.

[Title Page](#)[Abstract](#)[Introduction](#)[Conclusions](#)[References](#)[Tables](#)[Figures](#)[◀](#)[▶](#)[◀](#)[▶](#)[Back](#)[Close](#)[Full Screen / Esc](#)[Printer-friendly Version](#)[Interactive Discussion](#)

Date	Activities
I	27 Aug, 06:00 UTC
II	27 Aug, 13:00 UTC
III	29 Aug, 17:00 UTC
IV	3 Sep, 10:00 UTC
V	13 Sep, 14:00 UTC

Table 2. Overview of peak discharges exceeding $1 \text{ m}^3 \text{ s}^{-1}$ since 1969. For the rainfall depth and duration, the period between initial and peak discharge is considered.

Date	Rainfall depth [mm]	Rainfall duration [h]	Initial discharge [l s^{-1}]	Peak discharge [$\text{m}^3 \text{ s}^{-1}$]
27 Aug 2010	151.8	23	4	4.97
31 Dec 1993	36.2	14	300	2.99
17 Nov 1990	15.4	13	148	2.81
15 Sep 1998	33.3	15	361	2.13
1 Nov 1998	22.6	13	282	2.05
30 Dec 2002	37.6	23	161	1.84

- [Title Page](#)
- [Abstract](#)
- [Conclusions](#)
- [Tables](#)
- [◀](#)
- [◀](#)
- [Back](#)
- [Full Screen / Esc](#)
- [Printer-friendly Version](#)
- [Interactive Discussion](#)
- [Introduction](#)
- [References](#)
- [Figures](#)
- [▶](#)
- [▶](#)
- [Close](#)

Soil buffer limits flash flood response to extraordinary rainfall

C. C. Brauer et al.

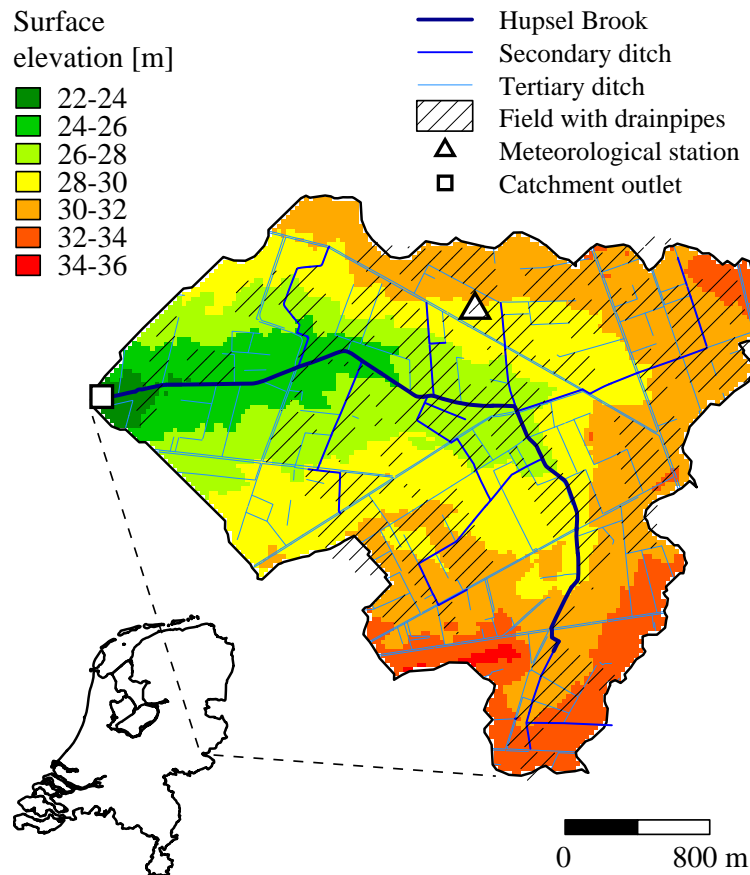


Fig. 1. Map of the Hupsel Brook catchment with the main hydrologically relevant features (adapted from Van der Velde et al., 2010).

Soil buffer limits flash flood response to extraordinary rainfall

C. C. Brauer et al.

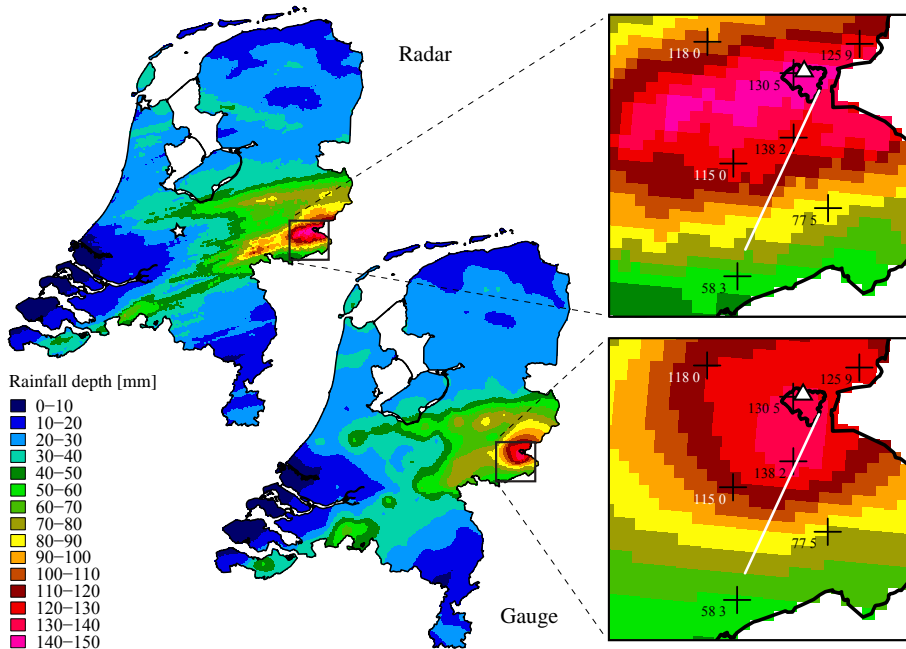


Fig. 2. Daily rainfall depths for 26 August, 08:00 UTC to 27 August, 08:00 UTC for The Netherlands and the region around the Hupsel Brook catchment. Upper panels: Depths for the gauge-adjusted radar composite. Lower panels: Depths for the interpolated manual rain gauge data. Also plotted are: weather radars (stars), manual rain gauges and their daily rainfall depths (crosses), automatic rain gauge (triangle), and microwave link path (line). Because the automatic rain gauge at Hupsel stopped recording at 21:00 UTC no daily rainfall depth was plotted for this gauge.

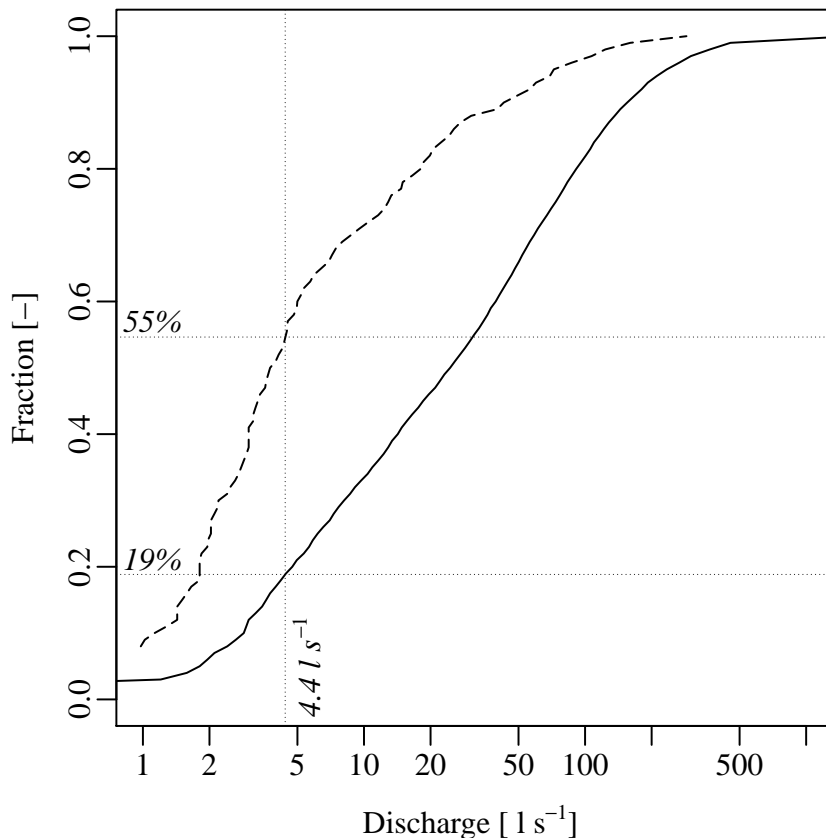


Fig. 3. Cumulative distribution functions of discharge at the catchment outlet. Solid: Based on all days between 1969 and 2010. Dashed: Based on all days in the last decade of August between 1969 and 2010. At the start of the rainfall event on 26 August 2010, discharge was 4.4 l s^{-1} .

Soil buffer limits flash flood response to extraordinary rainfall

C. C. Brauer et al.

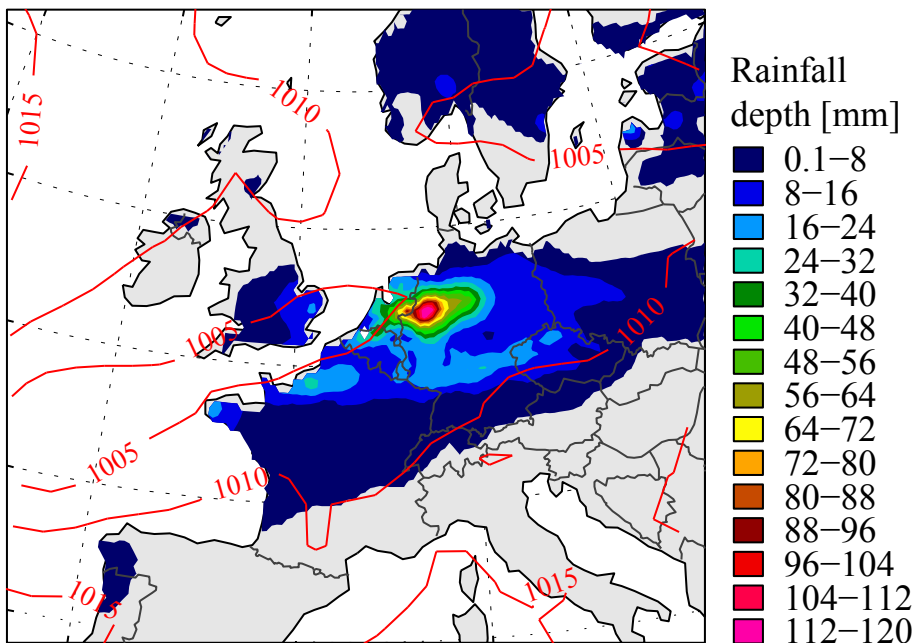


Fig. 4. Large-scale patterns of mean sea level pressure (hPa) and precipitation accumulation for 26 August 2010 (00:00–24:00 UTC). Pressure data come from the ERA Interim reanalysis (18:00 UTC). Precipitation is taken from the daily gridded observational dataset provided by the ECA&D (Haylock et al., 2008).

Title Page	
Abstract	Introduction
Conclusions	References
Tables	Figures
◀	▶
◀	▶
Back	Close
Full Screen / Esc	
Printer-friendly Version	
Interactive Discussion	

Soil buffer limits flash flood response to extraordinary rainfall

C. C. Brauer et al.

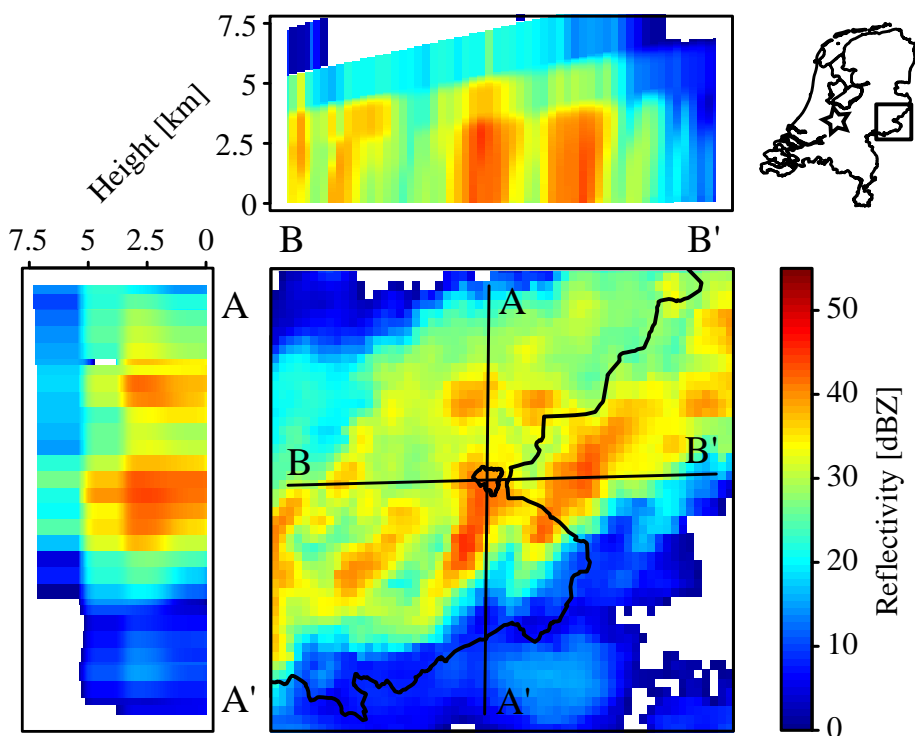


Fig. 5. Spatial variation in radar reflectivity for 26 August, 19:15 UTC. Reflectivity is derived from the 14-elevation volume scan of the KNMI weather radar in De Bilt (star). Side panels show the vertical distribution of the reflectivity for two transects over the Hupsel Brook catchment.

- [Title Page](#)
- [Abstract](#) [Introduction](#)
- [Conclusions](#) [References](#)
- [Tables](#) [Figures](#)
- [◀](#) [▶](#)
- [◀](#) [▶](#)
- [Back](#) [Close](#)
- [Full Screen / Esc](#)
- [Printer-friendly Version](#)
- [Interactive Discussion](#)

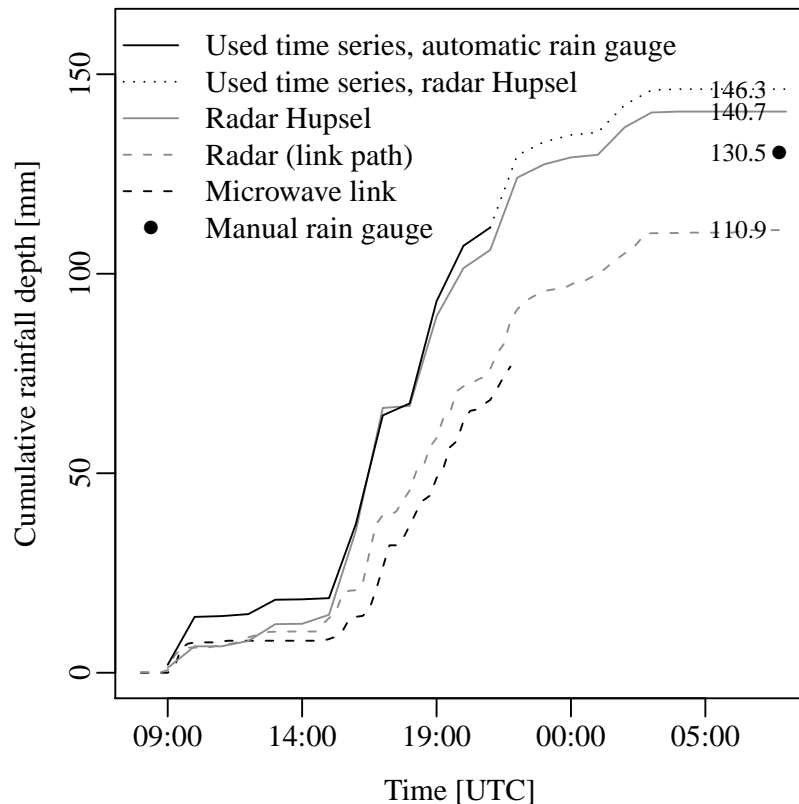


Fig. 6. Cumulative rainfall depths from 26 August, 08:00 UTC to 27 August, 08:00 UTC. Solid black: From automatic rain gauge. Dotted black: From gauge-adjusted radar data at the location of the automatic rain gauge, which were used to fill gaps of the automatic rain gauge data. Solid grey: gauge-adjusted radar data at the location of the automatic rain gauge. Dashed grey: gauge-adjusted radar data path-averaged over the microwave link path. Dashed black: microwave link. One black point: manual rain gauge.

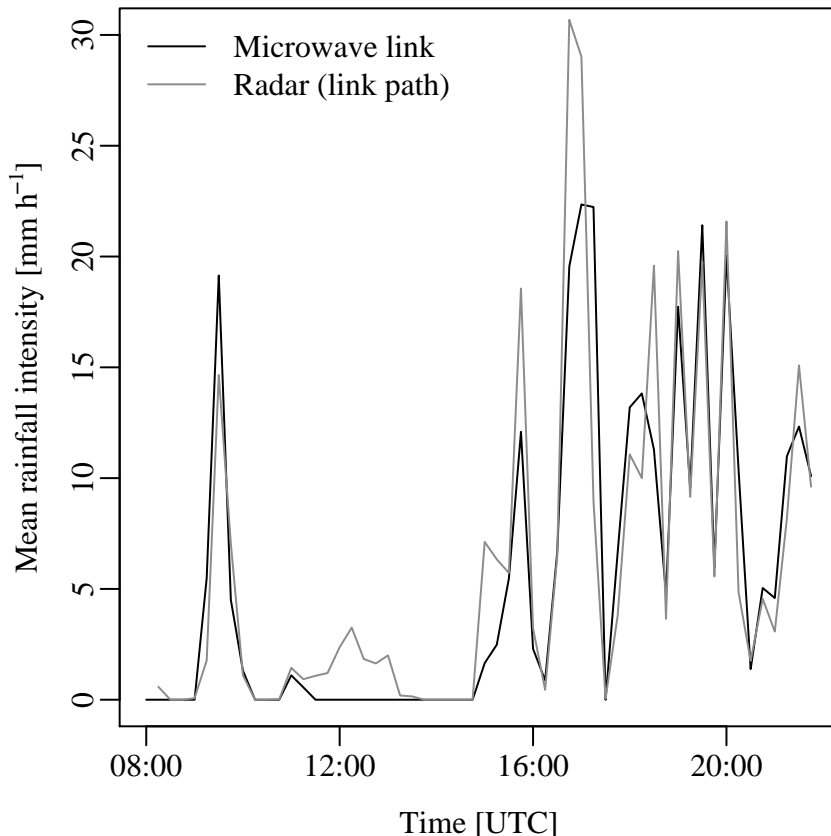


Fig. 7. Temporal dynamics of rainfall intensity on 26 August 2010 over the Hupsel Brook catchment. Rainfall is estimated from commercial microwave link data (black line) and path-averaged gauge-adjusted radar data (grey line). The temporal resolution is 15 min. Rainfall intensities from radar data are shifted 15 min forward in time, because it takes some time for the droplets measured up in the air by the radar to reach the level of the microwave link.

Soil buffer limits flash flood response to extraordinary rainfall

C. C. Brauer et al.

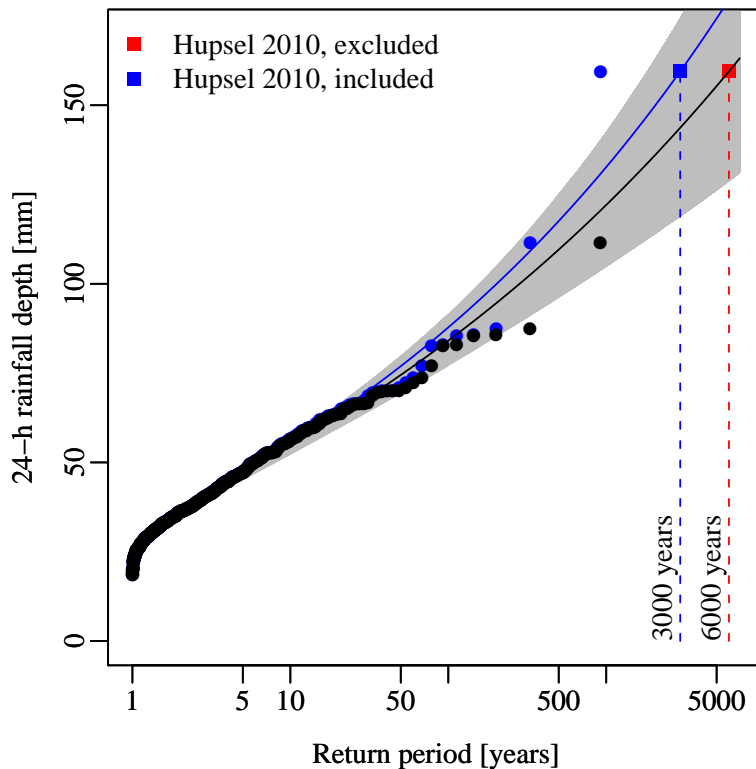


Fig. 8. Probability plot with the GEV distribution fitted to annual 24-h rainfall maxima. The method of L-moments was used (Hosking and Wallis, 1997). Dots: ordered annual maxima plotted with the Gringorton plotting position and lines represent GEV fits. Points in black: Obtained from Overeem et al. (2008), points in blue are based on the same 514-year data set including the recent Hupsel maximum of 159.5 mm. Red and blue squares: The 24-h accumulation of 159.5 mm and corresponding return periods. Grey-shaded area: The 95% confidence interval based on the bootstrap method.

Soil buffer limits flash flood response to extraordinary rainfall

C. C. Brauer et al.

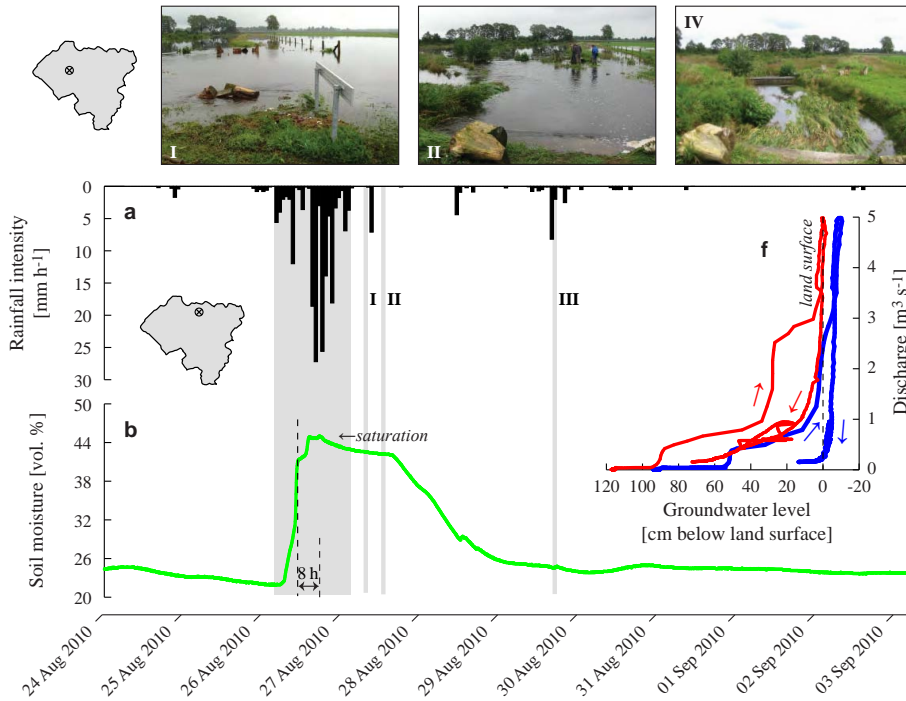


Fig. 9a. Hydrological response of the Hupsel Brook catchment to the 26 August 2010 rainfall. **(a)** hourly rainfall depths measured with the automatic rain gauge (gaps filled with radar estimates), **(b)** soil moisture content at 40 cm depth, **(c)** groundwater level in two piezometers, **(d–e)** discharge at the catchment outlet on logarithmic and linear axes, and **(f)** relation between discharge and groundwater depth. The roman numbers indicate the post-event field surveys (Table 1). The small catchment maps show (1) the location of the three upper photos, (2) the location of the rainfall, soil moisture and groundwater measurements and (3) the location of the catchment outlet and the three lower photos.

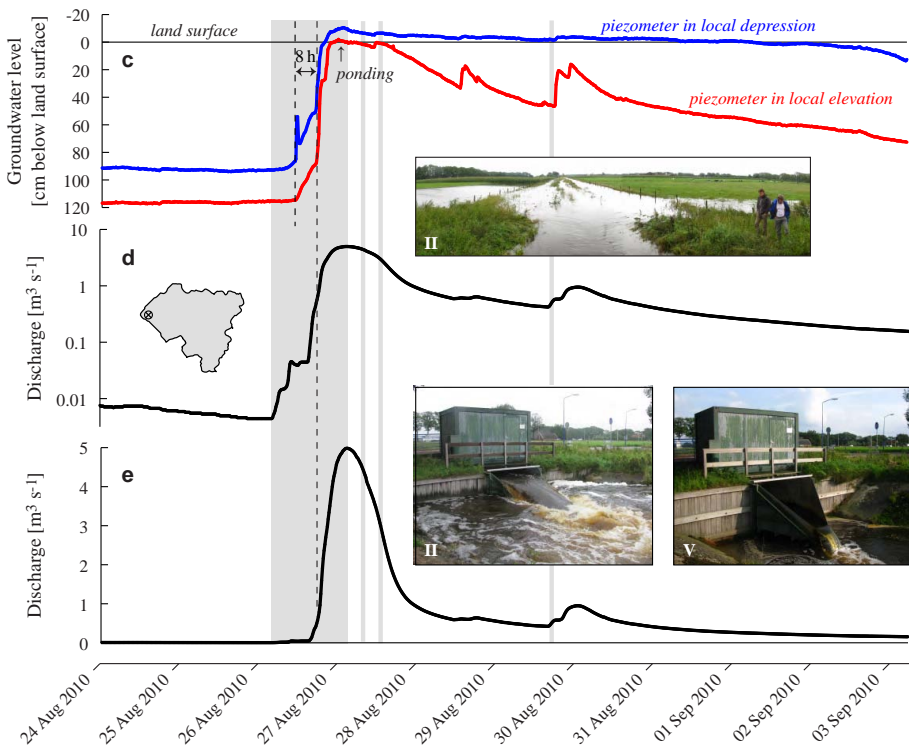


Fig. 9b. Continued.

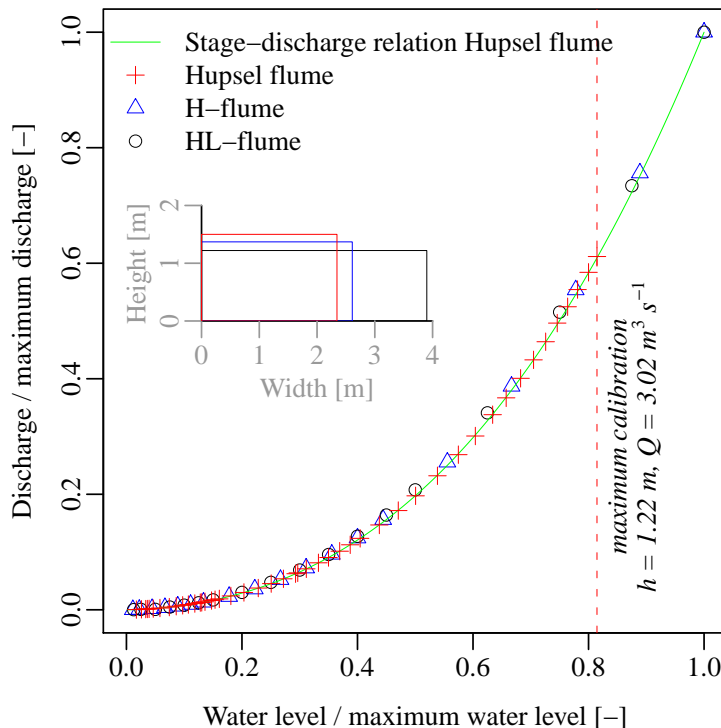


Fig. 10. Stage-discharge relationships for different types of H-flumes. Points: Calibration data of stage-discharge relationships of standard H- and HL-flumes and the flume at the outlet of the Hupsel Brook catchment. Line: The employed stage-discharge relationship for the Hupsel flume, extrapolated from $h = 1.22$ m. Water levels and discharges have been normalized with respect to their maximum values (Hupsel flume: $h_{\max} = 1.50$ m, $Q_{\max} = 4.94 \text{ m}^3 \text{ s}^{-1}$; H-flume: $h_{\max} = 1.37$ m, $Q_{\max} = 2.39 \text{ m}^3 \text{ s}^{-1}$; HL-flume: $h_{\max} = 1.22$ m, $Q_{\max} = 3.31 \text{ m}^3 \text{ s}^{-1}$). Calibration data of the H- and HL-flumes are taken from Kilpatrick and Schneider (1983). The inset shows the dimensions of the flumes.

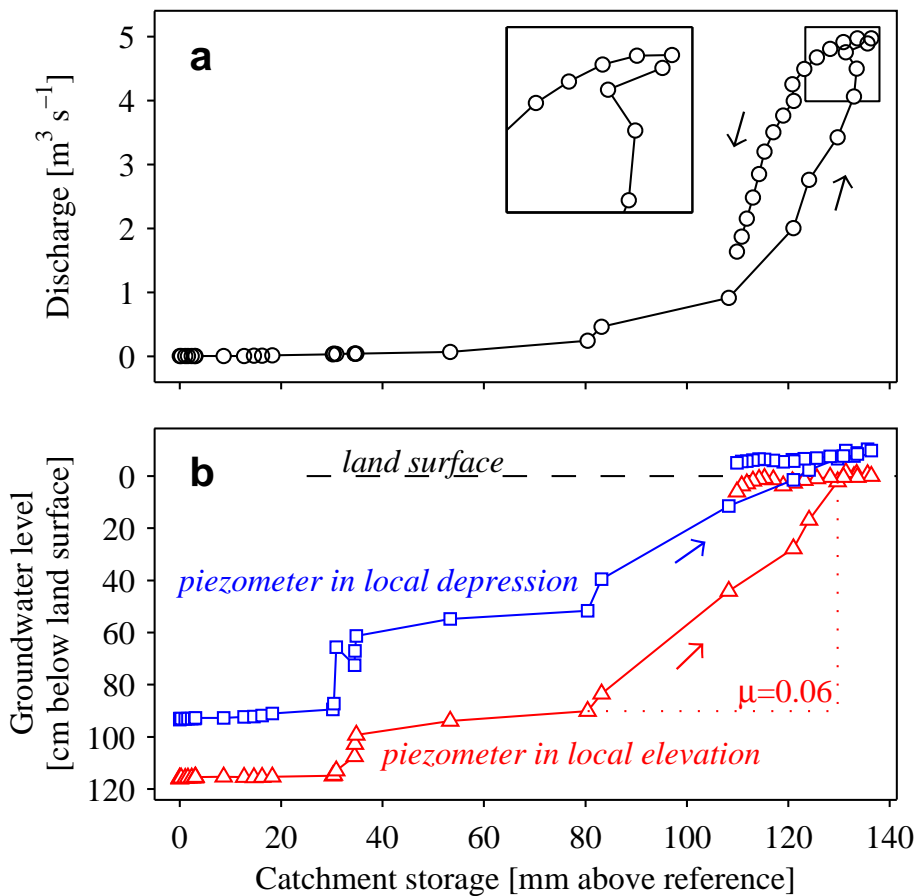


Fig. 11. Discharge at the outlet (upper panel) and local groundwater level (lower panel) as a function of estimated catchment storage for the period 25 August, 18:15 UTC to 27 August, 18:00 UTC. Points are drawn for each hour.

Soil buffer limits flash flood response to extraordinary rainfall

C. C. Brauer et al.



Fig. 12. The role of culverts during the 27 August 2010 flash flood. The roman numbers indicate the post-event field surveys (Table 1). Upper panels: Situation directly after the flood. Upwelling water reveals the exit of the submerged culvert. The resulting backwater feedback allows water to bypass the obstacle on the right by flowing over the road and the adjacent field back into the brook (arrows). Lower left panel: upstream entry of the culvert. Logs (black arrows) deposited by flood and flow marks in grass (upper left panel) indicate that water flew over the culvert at flood peak. Lower right panel: situation two weeks after flood with flood marks indicated. Photo's in top panels of Fig. 9 are taken from same location but in upstream rather than downstream direction.